RESEARCH ARTICLE

WILEY

Modulation of cortical beta oscillations influences motor vigor: A rhythmic TMS-EEG study

Kazumasa Uehara 1,2,3 | Justin M. Fine 1,4 | Marco Santello 1

Correspondence

Marco Santello, School of Biological and Health Systems Engineering, 501 East Tyler Mall, ECG Building, Suite 334, Arizona State University, Tempe, AZ 85287-9709, USA. Email: marco.santello@asu.edu

Funding information

National Science Foundation, Grant/Award Number: BCS-1827752

Abstract

Previous electro- or magnetoencephalography (Electro/Magneto EncephaloGraphic; E/MEG) studies using a correlative approach have shown that β (13–30 Hz) oscillations emerging in the primary motor cortex (M1) are implicated in regulating motor response vigor and associated with an anti-kinetic role, that is, slowness of movement. However, the functional role of M1 β oscillations in regulation of motor responses remains unclear. To address this gap, we combined EEG with rhythmic TMS (rhTMS) delivered to M1 at the β (20 Hz) frequency shortly before subjects performed an isometric ramp-and-hold finger force production task at three force levels. rhTMS is a novel approach that can modulate rhythmic patterns of neural activity. β -rhTMS over M1 induced a modulation of neural oscillations to β frequency in the sensorimotor area and reduced peak force rate during the ramp-up period relative to sham and catch trials. Interestingly, this rhTMS effect occurred only in the large force production condition. To distinguish whether the effects of rhTMS on EEG and behavior stemmed from phase-resetting by each magnetic pulse or neural entrainment by the periodicity of rhTMS, we performed a control experiment using arrhythmic TMS (arTMS). arTMS did not induce changes in EEG oscillations nor peak force rate during the rump-up period. Our results provide novel evidence that β neural oscillations emerging the sensorimotor area influence the regulation of motor response vigor. Furthermore, our findings further demonstrate that rhTMS is a promising tool for tuning neural oscillations to the target frequency.

KEYWORDS

cortical oscillations, motor control, primary motor cortex

1 | INTRODUCTION

Rhythmic neural activity is a fundamental feature of the central nervous system (CNS) (Buzsáki & Draguhn, 2004). β (13–30 Hz) oscillations are ubiquitously distributed throughout the whole brain, but are most predominantly observed in the sensorimotor area (Brittain & Brown, 2014; Brown, 2000; Engel & Fries, 2010). Within the primary

motor cortex (M1), β -power modulation occurs during preparation and execution of voluntary movements (Androulidakis et al., 2006; 2007; Ball et al., 2008; Cheyne et al., 2008; Muthukumaraswamy, 2010; Salenius et al., 1996). The notion of an anti-kinetic role of β oscillations (15–25 Hz frequency) is based on studies of Parkinson's disease patients who exhibit slowed movement or reaction times coinciding with heightened subcortical β power

This is an open access article under the terms of the Creative Commons Attribution-NonCommercial-NoDerivs License, which permits use and distribution in any medium, provided the original work is properly cited, the use is non-commercial and no modifications or adaptations are made.

© 2022 The Authors. *Human Brain Mapping* published by Wiley Periodicals LLC.

¹School of Biological and Health Systems Engineering, Arizona State University, Tempe, Arizona, USA

²Division of Neural Dynamics, Department of System Neuroscience, National Institute for Physiological Sciences, Okazaki, Aichi, Japan

³Department of Physiological Sciences, School of Life Science, SOKENDAI (The Graduate University for Advanced Studies), Okazaki, Aichi, Japan

⁴University of Minnesota Medical School, Minneapolis, Minnesota, USA

UEHARA ET AL. WILEY 1159

(Chen et al., 2007; David et al., 2005), β coherence between M1 and subthalamic nucleus (van Wijk et al., 2017), and increased β power desynchronization in M1 with changes in motor parameters such as force modulation for postural adjustments (see Bjorg et al., 2013 for review). However, these seminal findings were revealed by a correlative approach, whereas the relation between β neural oscillations to motor behavior has remained elusive.

To address this, several studies have leveraged a causal approach that combined noninvasive brain stimulation with electroencephalography (EEG), together with behavioral measures, to manipulate brain activity and quantify the relation between changes in neural oscillations and behavioral responses. For example, human studies using transcranial alternating current stimulation (tACS) have yielded mixed results by showing that tACS-induced β oscillations in M1 slow down motor actions (Pogosyan et al., 2009) or have no effect on motor responses (Moisa et al., 2016). A potential reason for these conflicting results is that these studies did not take into account the relation between M1 β oscillations and force magnitude. Changes in cortical β oscillations have been known to be sensitive to the magnitude of force output (Mima et al., 1999; Tan et al., 2015). This suggests that the relation between β cortical oscillations and motor responses may differ depending the magnitude of force production. Another reason why previous work using neuromodulation generated mixed results is that the spatial resolution of tACS might not be suitable to consistently elicit changes in neural oscillations and/or behavioral responses. The present study was designed to address both of these limitations by asking participants to generate different magnitudes of digit forces while being stimulated using rhythmic transcranial magnetic stimulation (rhTMS).

rhTMS is an approach that has been developed in the last decade to drive ongoing neural oscillations to the target frequency (Albouy et al., 2017; Chanes et al., 2013; Di Gregorio et al., 2022; Okazaki et al., 2021; Romei, Bauer, et al., 2016; Thut, Veniero, et al., 2011; Trajkovic et al., 2022; Vernet et al., 2019). It has been proposed that a modulation of neural oscillations induced by periodic external stimuli, that is, rhTMS, can lead to temporal realignment of rhythmic patterns of neural ensembles (Thut, Schyns, & Gross, 2011; see Thut, 2014 for review). Therefore, driving neural oscillations using rhTMS allows to establish whether neural oscillations at the stimulation frequency can causally drive behavioral responses, as opposed to these oscillations simply being an epiphenomenon.

By combining rhTMS and EEG we investigated whether, by modulating β oscillations in the sensorimotor area, $\beta\text{-rhTMS}$ (20 Hz) affected peak force rate during a force production task. Given that high β frequency has been associated with slowed movement in Parkinson's patients (Chen et al., 2007), we hypothesized that $\beta\text{-rhTMS}$ (20 Hz) would induce a decrease in peak force rate. To address whether this effect might be dependent on the vigor of force production, we applied that $\beta\text{-rhTMS}$ while subjects generated three levels of isometric finger forces. Moreover, to determine whether the hypothesized effects of $\beta\text{-rhTMS}$ on a modulation of neural oscillations and peak force rate are specific to β stimulation frequency, we tested a control condition using $\gamma\text{-rhTMS}$ (40 Hz). Based on previous work

(Ball et al., 2008; Cheyne & Ferrari, 2013; Santarnecchi et al., 2017), low γ -frequency (approximately 40 Hz) stimulation should have no effect on motor responses, as these effects appear to be limited to high γ -rhTMS frequencies (>70 Hz).

We conducted an additional experiment to control for the possibility that rhythmic TMS-related neural and behavioral effects may be merely driven by the wideband phase-locking changes that can occur through either single or multiple rapid TMS pulses (Herring et al., 2015). For this second experiment, we used arrhythmic TMS (arTMS), which has been previously shown to effectively distinguish rhythmic TMS-specific from nonspecific effects on neural and behavioral responses (Thut, Veniero, et al., 2011). We expected that arTMS should not cause a modulation of the targeted cortical oscillations nor changes in motor responses hypothesized for the $\beta\text{-rTMS}$ condition.

2 | MATERIALS AND METHODS

2.1 | Subjects

Twenty-eight healthy young volunteers (mean age 23.5 years, standard deviation [SD] 3.6 years; 6 females; all right-handed, self-reported) without history of musculoskeletal or neurological disorder participated in Experiment 1 (rhythmic TMS, rhTMS). Nine additional subjects (mean age 27.0 years, SD 5.3 years; 5 males) were recruited in Experiment 2 (arrhythmic TMS, arTMS). Subjects were screened for contraindications to TMS in accordance with TMS safety guidelines (Keel et al., 2000; Rossi et al., 2009). Arizona State University Ethics Committee approved this study in accordance with the guidelines established in the Declaration of Helsinki and written informed consent was obtained from all subjects. For Experiment 1, subjects were randomly assigned to the β-rhTMS (mean age 22.6 years, SD 1.7 years; 2 females) or γ-rhTMS (mean age 24.3 years, SD 4.7 years; 4 females) group (n = 14 each). For Experiment 2, all subjects received β- and γ-arTMS.

2.2 | Experimental task and protocols

All subjects were naïve to the purpose of the study. Subjects sat upright on a comfortable chair with their right forearm supported by a rigid table and their head laying on the chair's headrest. Subjects' head was stabilized by a forehead rest to ensure a consistent position throughout the duration of the experimental session.

Subjects wore earplugs throughout data collection to minimize the effects of TMS sounds on motor behavior and brain activity.

We chose to study a force control task (ramp-up and hold) based on literature showing a relation of motor β -frequency to action vigor (e.g., velocity of movement) (Brucke et al., 2012; Joundi, Brittain, et al., 2012; Moisa et al., 2016; Pogosyan et al., 2009). Therefore, in our study we focused on changes in peak force rate that might have been induced by β -rhTMS.

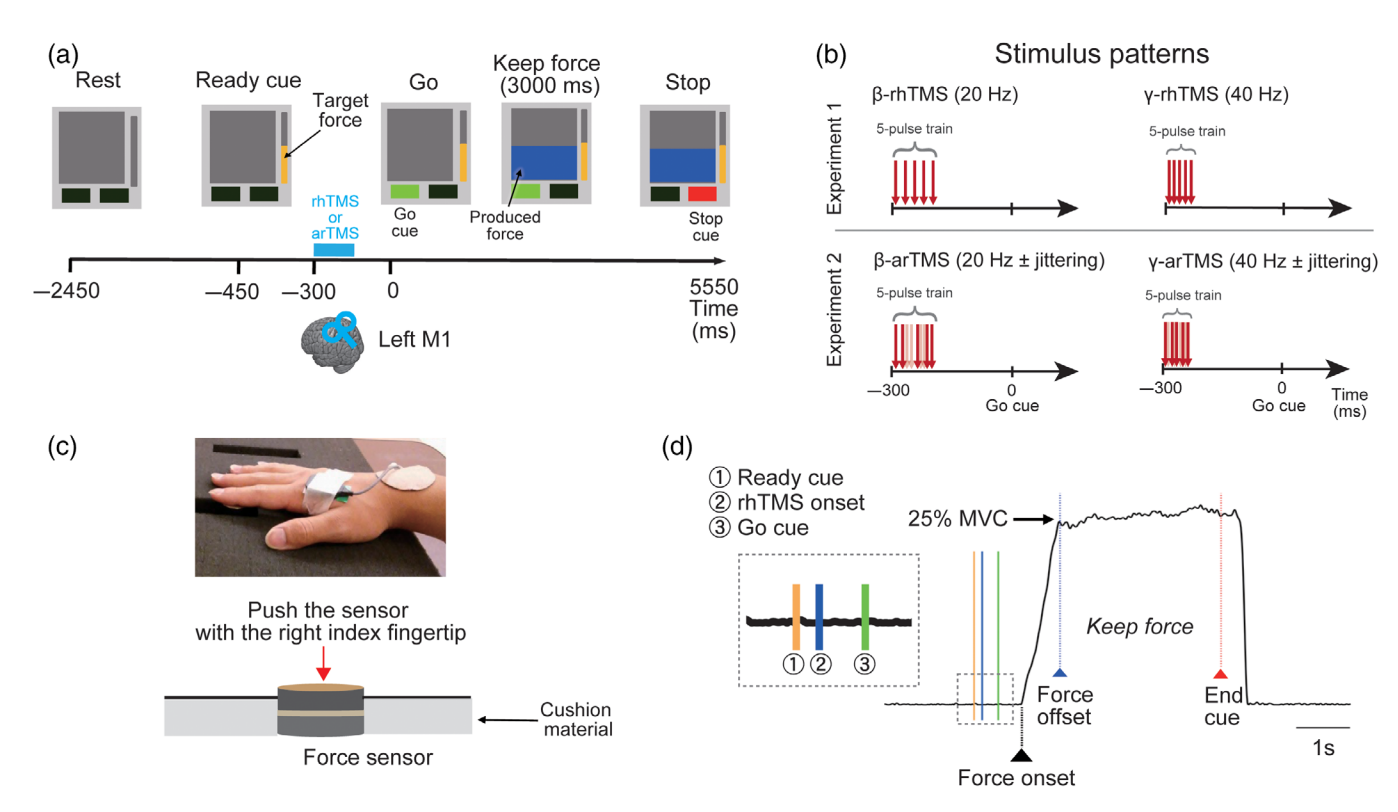


FIGURE 1 Trial structure and force production task. (a) Subjects were instructed to perform a visually-guided force production task to match one of three different targets (5%, 10%, and 25% of MVC) by pressing a force-torque transducer with their right index fingertip. After 2 s from the visual "Rest" cue, the target force level was displayed on the monitor (i.e., "Ready" cue). Rhythmic TMS (rhTMS) and arrhythmic TMS (arTMS) for Experiment 1 and 2 were applied over left M1 through short burst of 5 pulses in a subset of trials 300 ms prior to visual "Go" cue (sky-blue horizontal line). After receiving the visual "Go" cue, subjects were asked to press on the force sensor with their index fingertip for 3 s throughout the "Keep force level" cue at the required force level as quickly and accurately possible. After receiving the visual "End" cue, subjects were asked to release the index fingertip from the force sensor and relax their right hand. (b) Stimulus pattens of rhTMS and arTMS. In rhTMS, five consecutive magnetic pulses were applied at 20 and 40 Hz. In arTMS, the timing of 2nd to 4th magnetic pulses were randomly jittered with an across-trial mean frequency of either 20 or 40 Hz depending on the stimulation condition. (c) Subject's hand posture during the data collection and a device instrumented with force/torque sensor. This sensor detects the load along Z-axis. (d) Typical force time course and trial events: "Ready" cue, rhTMS onset, and "Go" cue

On each trial, we instructed subjects to perform a visually-guided force production task consisting of a ramp (dynamic) and hold (static) phase. A visual display cued subjects about the force target, as well as onset and offset of force production (Figure 1a). The display also provided online feedback of force output throughout the trial. Two seconds after the visual "Rest" cue, the target force was displayed as an orange vertical bar (i.e., "Ready" cue, Figure 1a). After 150 ms from the "Ready" cue, we applied rhTMS (Experimental 1) and arTMS (Experimental 2) over the left primary (M1) representation of the right first dorsal interosseous muscle (FDI) (see Rhythmic TMS procedures) (Figure 1b). Subjects were required to press a force sensor (Nano 25, ATI Industrial Automation, Garner, NC; nominal force resolution: 0.012 N) along the Z-axis (red arrow, Figure 1c) with the right index fingertip to reach one of three force targets for 3 s (5%, 10%, and 25% of maximal isometric voluntary contraction, MVC). Before the experimental task, subjects performed three MVC trials using their right index finger. Each subject's largest force was defined as MVC and used to determine individual target forces of 5%, 10%, and 25% of MVC (see example of 25% MVC force trace, Figure 1d).

In Experiment 1, we randomly assigned 28 participants to the β -rhTMS and γ -rhTMS groups (14 participants in each group). The β -rhTMS and γ -rhTMS groups received a 5-magnetic pulse train that lasted 250 and 125 ms, respectively. This design was motivated by the need of using the same number of TMS pulses in both groups (5 pulses of each trial) to enable a between-group comparison while adhering to TMS safety guidelines regarding the total number of TMS stimuli. Based on these considerations, we chose not to use the alternative approach of using rhTMS over the same period of time in both groups, as this would have led to delivering a number of pulses in the γ -rhTMS group above the safety threshold guidelines (Rossi et al., 2009). For Experiment 2, we used the same experimental protocol used for Experiment 1, with the only exception being that we applied a different stimulation protocol.

In both Experiments 1 and 2, we delivered TMS over M1 immediately before movement onset, that is, "Go" cue (Figure 1a,b and d)

10970193, 2023, 3, Downloaded from https://onlinelibrary.wiley.com/doi/10.1002/hbm.26149, Wiley Online Library on [25/01/2023]. See the Terms and Conditions (https://onlinelibrary.wiley.com/terms-and-conditions) on Wiley Online Library for rules of use; OA articles are governed by the applicable Creative Commons. Licensee

based on observations that neural oscillations in the β - and γ -frequency bands (approximately 15–30 and 60–90 Hz, respectively) reliably occur in motor-related brain areas during movement preparation (Ball et al., 2008; Khanna & Carmena, 2017; Pfurtscheller & Lopes Da Silva, 1999; Salenius et al., 1996; Tzagarakis et al., 2010, 2015). Visual cues and timing of the TMS onset were controlled by custom-written script implemented in LabVIEW software (version 2015, National Instruments, Austin, TX).

2.3 | Experiment 1: Rhythmic TMS

Subjects completed two experimental conditions (rhTMS and sham) in the same session, with a counter-balanced order across subjects. For the rhTMS condition, subjects performed 40 trials with rhTMS and 15 trials with no rhTMS (i.e., catch trials) for each target force level (total of 165 trials), rhTMS and catch trials were presented in a randomized order within the rhTMS condition. The sham condition consisted of trials where subjects heard the TMS sound but received no stimulation (40 trials) and 15 trials with no sound (catch trials) for each target force level (165 trials). The sham and catch trials were also presented in a randomized order within the sham condition. Sham trials were used as a control condition to rule out placebo effects that might have been caused by the TMS click sound (Nikouline et al., 1999). Catch trials were used to rule out potential effects of auditory and stimulation of scalp skin afferents on force production. With the exception of lack of stimulation, the procedures for the sham condition were identical to those above described for the rhTMS condition. Hence, each subject performed a total number of 330 trials.

2.4 | Experiment 2: Arrhythmic TMS

In Experiment 1, we found that peak force rate was significantly modulated by five consecutive magnetic stimuli at the β -frequency band. However, this behavioral response modulation could have been caused by two alternative mechanisms: one that is specific to the rhythmic stimulation frequency we used (β), or a mechanism that is nonfrequency specific and related only to the number of consecutive magnetic pulses. Experiment 2 was designed to distinguish between these two mechanisms. The only differences between the protocol of Experiment 2 and 1 were: (1) we used a within-subject design that involved subjects generating two levels of force (5% and 25% MVC); and (2) subjects performed three types of trials: catch trials (no stimulation), arrhythmic β TMS, and arrhythmic γ TMS. TMS conditions and catch trials were presented in a randomized order.

We did not include a sham session as this was used in Experiment 1. Furthermore, we sought to maximize the statistical power of comparing arrhythmic β with arrhythmic γ while avoiding excessively long experimental sessions that could have induced fatigue. As done in Experiment 1, the TMS conditions consisted of 40 trials for each target force level and TMS frequency, thus yielding a total of 160 TMS trials. We used 15 catch trials for each target force level, for a total of

30 catch trials. Therefore, the whole experiment consisted of 190 trials.

2.5 | Rhythmic TMS procedures (Experiment 1)

In order to manipulate ongoing neural oscillations, we used a rhTMS paradigm that has been found to selectively control the interplay between endogenous oscillatory neural activity and magnetic forces at the stimulated frequency (Thut, Veniero, et al., 2011; Romei, Bauer, et al., 2016; Albouy et al., 2017; for review see Farzan et al., 2016; Romei, Thut, & Silvanto, 2016). rhTMS and sham (i.e., coil perpendicular to the scalp) were delivered with a figure-of-eight coil (wing diameter: 70 mm) connected to a Magstim rapid² biphasic stimulator (Magstim Company, Dyfed, UK). To define stimulus parameters, surface electromyographic (EMG) activity was recorded from the first dorsal interossues (FDI) of the subject's right hand through active bipolar surface electrodes (Delsys, Inc., Boston, MA) following standard skin preparation. EMG signals were amplified (×1000; Delsys Bagnoli amplifier system), band-pass filtered (10-1000 Hz), sampled at 5 kHz (Micro 1401; Cambridge Electronic Design, Cambridge UK), and stored to a computer via Signal software (Cambridge Electronic Design, Cambridge UK) for offline analysis. The optimal site for producing MEPs in the FDI of the right hand was determined using standard procedures (Chipchase et al., 2011) and marked on the EEG cap over the subject's scalp (see below). Active motor threshold (AMT) for the right FDI was then defined as the minimum intensity that elicited MEPs of at least 100 µV in 5 out of 10 trials during a weak sustained isometric muscle contraction of the right FDI (~10% MVC). Intensity of rhTMS was set to 90% of AMT (Romei, Bauer, et al., 2016). β-rhTMS was applied at 20 Hz through a 5-magnetic pulse train (inter-stimulus interval: 50 ms) over the left M1 for 250 ms. We also applied rhTMS at 40 Hz to the same brain area, which corresponds to low-y frequency, through a 5-magnetic pulse train (inter-stimulus interval: 25 ms) for 125 ms. This means that one stimulus train (i.e., a 5-magnetic pulse train) was delivered on each experimental trial (Figure 1a,b). For brevity, we will use the term "γ-rhTMS" throughout the manuscript to denote the 40 Hz stimulation. For all TMS sessions, the coil was placed tangentially to the scalp with the handle pointing backwards at a 45° from the sagittal plane. For the sham session, the coil was placed perpendicularly to the scalp over the right M1. These TMS procedures are consistent with safety guidelines regarding stimulation parameters such as intensity, total number of pulses, and ethical guidelines (Rossi et al., 2009).

2.6 | Arrhythmic TMS procedures (Experiment 2)

This experiment was designed to control for the possibility that the rhTMS protocol (Experiment 1) can exert effects on behavioral responses and underlying "oscillatory" mechanisms through the propagation of single pulses either at the beginning or end (or both) of a rapid pulse train (Chanes et al., 2013). Specifically, even a single TMS

10970193, 2023, 3, Downloaded from https://onlinelibrary.wiley.com/doi/10.1002/hbm.26149, Wiley Online Library on [25/01/2023]. See the Terms and Conditions (https://onlinelibrary.wiley.com/terms-and-conditions) on Wiley Online Library for rules of use; OA articles are governed by the applicable Creative Commons. Licensee

pulse has been shown to exhibit a frequency broadband effect on neural oscillatory measures of power and phase-locking (Herring et al., 2015). Thus, the arrhythmic approach provides a control to examine the putative oscillatory nature of neural mechanisms because only rhythmic, but not arrhythmic, TMS should disrupt their phasic properties (Thut, Veniero, et al., 2011). Unless otherwise stated, procedures for Experiment 2 were the same as those used for Experiment 1. The most critical difference between Experiment 2 and 1 was that we delivered a form of arrhythmic stimulation at both β and γ frequencies that allowed us to quantify the effects an initial and final single pulse might have had on behavioral and neural outcomes. We note that arrhythmic stimulation still involved applying a train of 5 pulses, wherein the 3 pulses occurring after the 1st one (pulse 2 through 4) were randomly jittered with an across-trial mean frequency of either β or γ depending on the stimulation condition.

2.7 | Data recording

2.7.1 | Electroencephalography

To record brain oscillatory activity throughout the experimental task, we used TMS-compatible EEG equipment (eego sports, Advanced Neuro Technology, Netherlands). EEG was continuously recorded from 63 scalp electrodes with the ground electrode placed at AFz and in accordance with the 10/10 layout using a TMS-compatible EEG cap (WaveGuard EEG cap). Electrooculography (EOG) was also recorded using electrodes placed above and below the left eye for monitoring vertical eye movements, and below the left and right eyes for monitoring horizontal eye movements. EEG signals were amplified and digitized with 24-bit resolution, and sampled at 2 kHz. Skin/electrode impedance was maintained below 5 k Ω throughout data collection.

2.7.2 | Force recording

Force data were acquired at sampling rate of 1 kHz using customwritten script implemented in LabVIEW software.

2.8 | Data analysis

2.8.1 | Force data

Force data were first low-pass filtered using a fifth order zero-lag Butterworth filter with 20 Hz cut off. Force onset was then defined for each trial as the first time point at which the signal exceeded a threshold (0.2 N) for at least 15 ms. The time at which subjects reached the target force (force offset) was defined as the time at which force exceeded the instructed target force for at least 15 ms. The force ramp phase was defined as the interval between force onset and offset. The force hold phase was defined as the 2-s period starting 1 s after force offset. Peak force rate during ramp-up phase was

calculated for each trial. These data were averaged within each experimental condition before averaging across subjects.

2.8.2 | EMG data

To check whether rhTMS caused involuntary muscle twitching, we analyzed EMG activity of the right FDI 200 ms before the "ready" cue and during the rhTMS epoch using custom-written Matlab code (version R2016a, MathWorks, Natick, MA). Specifically, we first computed the root-mean squared (RMS) of EMG activity over the 200-ms window before the 'ready' cue (baseline EMG RMS). We then excluded trials for which EMG activity during the rhTMS epoch (250 and 125 ms for beta and gamma rhTMS, respectively) was greater than 2 standard deviations of baseline EMG RMS. Trials were excluded if EMG RMS amplitude during rhTMS was greater than 2 standard deviations of baseline EMG RMS. The application of this criterion led to the exclusion of very few trials from analysis (1.1% of total trials), thus indicating that delivery of rhTMS over M1 very rarely caused muscle twitching.

2.8.3 | EEG data

EEG analysis was performed using functions form the EEGLAB toolbox (Delorme & Makeig, 2004) in combination with custom-written Matlab code. With regard to preprocessing and artifact removal, EEG signals were first re-referenced to common average reference. After this step, the EEG data were segmented into 8 s epochs from 2.45 s before to 5.55 s after the "Go" cue. Previous TMS-EEG literature has reported that the duration of TMS-induced artifacts typically lasts relative to each magnetic pulse (Veniero et al., 2009). Based on this literature, to remove EEG artifacts caused by each TMS pulse we used linear interpolation of EEG data for a 15-ms time window from 2 ms before to 13 ms after each TMS pulse. After removing TMS artifacts, the interpolated EEG data were band-pass filtered between 1 and 70 Hz, and 60 Hz power line noise was removed. Subsequently, the filtered EEG data were down sampled to 1 kHz. To remove the remaining artifacts associated with eye movements, eye blinks, and muscle contractions, we applied independent component analysis (ICA). Components reflecting artifacts were then selected by visual inspection based on previous reports (Radüntz et al., 2015; Romero et al., 2008). After performing ICA, epochs containing residual artifacts were detected using an amplitude criterion (±100 μV) and were excluded from subsequent analysis. Finally, in the last step, to reduce the effects of volume conduction, we applied current source density transformation using the current source density (CSD) toolbox (version 1.1), which is based on the spherical spline algorithm (Kayser & Tenke, 2006; Perrin et al., 1989). Artifact-corrected epochs were therefore used for subsequent analysis. Note that the same preprocessing pipeline was applied to each condition (rhTMS, sham, and catch). Consequently, 8.2% of the trials across all subjects were excluded from the final analysis due to EEG noise issues.

To identify time-frequency EEG phase, time-frequency representations of single-trial EEG signals were calculated using complex Morlet's wavelet (Tallon-Baudry et al., 1996). The CSD-transformed EEG signals were first convoluted by a Morlet's wavelet function w(t,f):

$$w(t, f) = A \cdot \exp\left(-\frac{t^2}{2\sigma_t^2}\right) \exp(i2\pi f t), \tag{1}$$

where t is time points, f is the center frequency, and σ is the standard deciation of the Gaussian window. $A = \left(\sigma_t \pi^{1/2}\right)^{-1/2}, \ \sigma_t = 1/(2\pi\sigma_t),$ and $\sigma_f = f/6$. We set the number of cycles to $(n_{co}) = 6$ and obtained the instantaneous phase (t,f) and amplitude (t,f) as f increased from 1 to 50 Hz in 1-Hz steps (Lachaux et al., 2000). Subsequently, to quantify the extent to which rhTMS locked ongoing neural oscillations, we calculated the phase synchrony across trials, that is, inter-trial phase coherence, by computing the phase locking factor (PLF) (Tallon-Baudry et al., 1996). In other words, PLF indexes the degree of phase entrainment with periodic external inputs, that is, rhTMS. PLF was calculated at each electrode (ch), time (t) and frequency (f) as follows:

PLF
$$(t, f, ch) = \frac{1}{n} |\sum_{n=1}^{N} \exp(i\varphi(t, f, ch, n))|,$$
 (2)

where φ is the instantaneous phase of EEG signals and N is the total number of epochs. Moreover, to minimize a bias in calculating the number of epochs, the PLF was transformed to Rayleigh's Z-values (hereafter referred to as zPLF) (Fisher, 1995; Kawasaki et al., 2014; Mazaheri & Jensen, 2006) at each electrode (*ch*), time (t) and frequency (*f*) as follows:

$$zPLF(t, f, ch) = N * PLF^{2}.$$
 (3)

Our main EEG analysis focused on the epoch during four oscillatory cycles immediately after rhTMS (i.e., 200 and 100 ms windows for β - and γ -rhTMS, respectively). As previous seminal human studies found rhTMS-induced EEG entrainments lasting for a few oscillatory cycles even after the end of rhTMS (Lin et al., 2021; Okazaki et al., 2021; Thut, Schyns, & Gross, 2011), we also focused on the four oscillatory cycles after the fifth (last) TMS pulse as a time window of interest in this study. After epoching, we averaged the epoched zPLF values at each EEG channel according to the bandwidths for β (18–25 Hz) and γ (38–45 Hz). Individual topological maps representing the zPLF values were used for statistical analyses.

To assess the relation between phase locking (zPLF changes) in the rhTMS condition and EEG oscillatory activity, we calculated time-frequency EEG power for catch trials to identify brain oscillatory activity using obtained instantaneous amplitudes (*t*,*f*). We performed this analysis to test the assumption that the effect of rhTMS on EEG entrainment depends on whether targeted neural oscillation is already in-phase or not with rhTMS. For example, if the targeted neural oscillation is in-phase, rhTMS cannot further enhance EEG phase synchronization due to a ceiling effect. EEG power was transformed into dB values by normalizing it to baseline power computed over a 2-s time

window before the 0.3 s relative to "Go" cue. A decrease and increase in dB-transformed EEG power reflect event-related desynchronization (ERD) and synchronization (ERS), respectively.

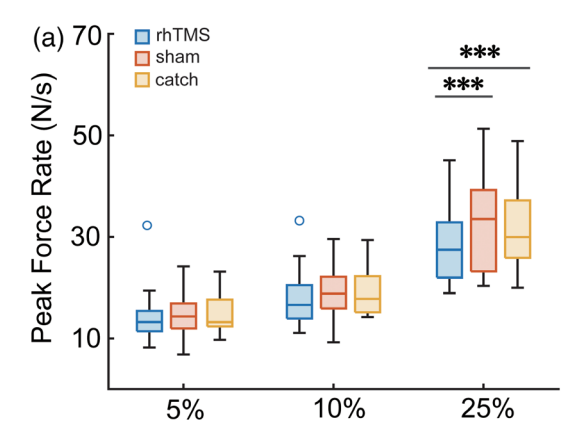
2.9 | Statistical analysis

Statistical analyses for the behavioral response and EEG data were implemented using R environment (R Development Core Team, version 3.4.1, www.r-project.org/). To test effects of manipulation of neural oscillations with β -, γ -rhTMS or arrhythmic TMS on peak force rate, we used linear mixed-effects modeling (West et al., 2007) with the Ime4 package (Pinheiro et al., 2017). p-Values for model effects were obtained using ImerTest package (Kuznetsova et al., 2016). This approach was chosen because mixed-effect modeling allows unbalanced data and missing observations, and considers individual variability of observations (Krueger, 2004). Each individual subjects' peak force rate during the ramp-up phase for each artifact-free trial was put into the model. For Experiment 1, GROUP (2 levels: β-, γ-rhTMS), FORCE LEVEL (3 levels: 5%, 10%, 25% MVC), STIMULATION TYPE (3 levels: rhTMS, sham, catch) and their interactions were treated as fixed factors in the model. The model also contained Subject level random intercepts. For Experiment 2, an experimental protocol and skipped a few conditions due to the limitation of the total duration of data collection. Due to methodological differences from Experiment 1, we used a within-subject design that reflected subjects experiencing (1) two levels of force (5% and 25% MVC) and (2) three types of trials (β -, γ -arrhythmic TMS, and catch). Therefore, STIMULATION TYPE (3 levels: β-arrhythmic TMS, γ-arrhythmic TMS, and sham), FORCE LEVEL (2 levels: 5%, 25% MVC) and their interactions were treated as fixed factors in the model. Followup comparisons for models yielding significant effects (or interactions) were conducted on the estimated marginal means using ImerTest package (Kuznetsova et al., 2016).

For EEG data from Experiment 1, significant differences in the zPLF values between the rhTMS and sham conditions were determined by using nonparametric, cluster-based permutation test (Maris & Oostenveld, 2007). This approach is able to control the large number of multiple comparison problem present in EEG datasets. To determine differences in zPLF between the rhTMS and sham conditions, we used a two-tailed paired t-test at each MVC condition. Here, we set total 5000 random permutations. For Experiment 2, we used two-tailed paired t-test at each MVC condition to compare zPLF in the arTMS and catch conditions. We performed a smaller number of random permutations (n = 512) due to the smaller number of subjects relative to Experiment 1. Statistically significant differences were tested at p < .05 as the cluster-statistical significance threshold for all EEG analyses.

3 | RESULTS

None of the subjects reported adverse effects and events associated with our TMS protocol during or after the experiments.



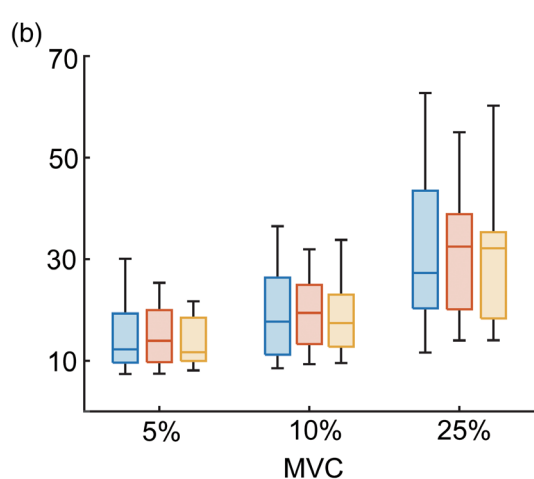


FIGURE 2 Peak force rate. Group-averaged peak force rate for each target force and trial type for the β - and low γ -rhTMS groups (a and b, respectively). Boxplots depict median (crossbar) and minimum and maximum values (whiskers). Open circles denote outlier. Statistically significant differences were determined using a liner-mixed model. *** denote statistically significant differences at p < .001.

3.1 | Experiment 1: Rhythmic TMS

3.1.1 | Behavioral results

RhTMS did not elicit muscle twitches in the right FDI since stimulation was delivered over M1 before the onset of voluntary muscle contraction and the stimulus intensity was set at 90% AMT. Therefore, muscle twitches did not affect our behavioral results. The mean peak force rate values for all conditions are shown in Figure 2a,b for the β -and γ -rhTMS groups, respectively. Using the mixed effects modeling, we found a significant main effect of FORCE LEVEL ($F_{[2, 451,743]} = 2114.86$, $p = 2.2 \times 10^{-16}$), STIMULATION TYPE ($F_{[2, 1857]} = 8.69$, $p = 1 \times 10^{-4}$), and a significant interaction between GROUP, FORCE LEVEL and STIMULATION TYPE ($F_{[4, 1107]} = 2.59$, p = .03), but no main effects of GROUP ($F_{[1, 3]} = 0.02$, p = .87). β -rhTMS led to a significant decrease in peak force rate at 25% MVC compared to the Sham (t = 7.92, p = .001) and Catch (t = 5.86,

p=.001) conditions, but not $\gamma\text{-rhTMS}$ condition. No significant differences in peak force rate were found at the 5% and 10% MVC condition irrespective of stimulation types (all p>.05). These results indicate that $\beta\text{-rhTMS}$ slowed down peak force rate, and this effect was conditional on the required target force level, the greatest effect being found at 25% MVC.

3.2 | EEG results

3.2.1 | Experiment 1: Phase locking factor

Time-frequency representations of z-transformed PLF (zPLF) around the onset and offset of rhTMS are shown in Figures 3a and 4a for β -and γ -rhTMS conditions, respectively. Figure 3a shows a group-averaged time-frequency representations of zPLF at the C3 channel in the 25% MVC condition. Figure 3b shows group-averaged topological maps representing β -band (18–25 Hz) zPLF in the β -rhTMS and sham conditions during 4 oscillatory cycles immediately after the end of fifth TMS pulse, calculated by cluster-based permutation tests. β -rhTMS significantly increased β -band zPLF relative to sham in the 25% MVC condition, but not in the 5% and 10% condition (p < .05, cluster-based comparison). Significantly greater β -band zPLF was broadly distributed around the contralateral and ipsilateral sensorimotor areas, compared to the sham condition, in particular for the 25% MVC condition (Figure 3b, t-map).

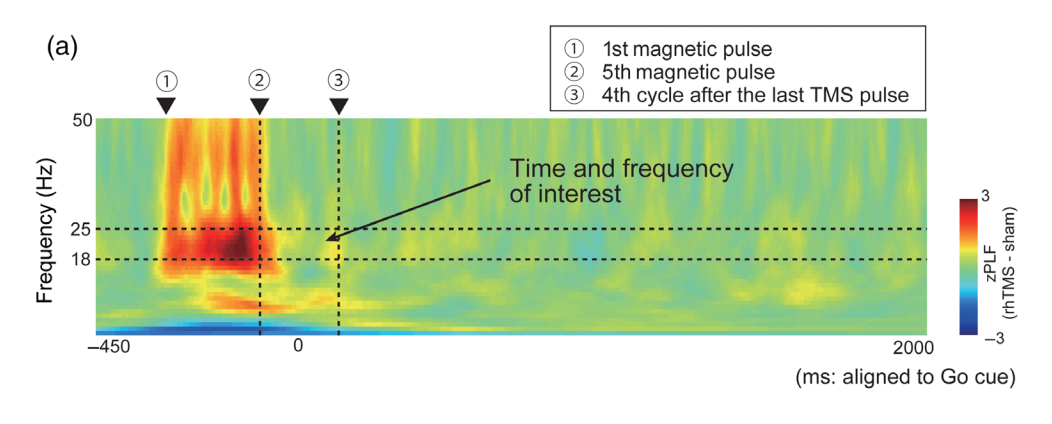
Figure 4a shows a group-averaged time-frequency representation of zPLF at C3 channel in the 25% MVC condition. Figure 4b shows group averaged topoplots representing γ -band (38–45 Hz) zPLF in the γ -rhTMS and sham conditions. When examining γ -rhTMS, we found a significant decrease in γ -band zPLF relative to the sham condition only in the 25% MVC condition, which was particularly evident in the occipital brain region (p < .05, cluster-based comparison; t-statistical map, Figure 4b).

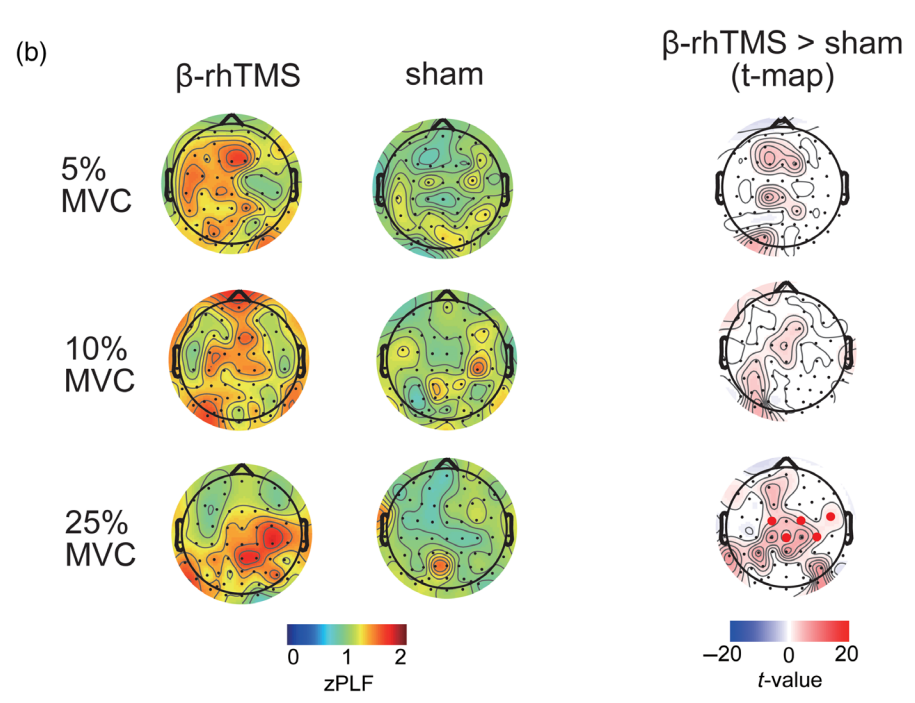
3.2.2 | Force-dependent changes in rhTMS-induced EEG entrainments

In the present study, β -rhTMS led to changes in both zPLF and peak force rate only in the 25% MVC condition. Here, another important question arises as to why neural and behavioral changes occurred only under the high force condition. To address this question, we calculated event-related desynchronization/synchronization (ERD/S) during same rhTMS time window (-300 to -50 ms before the "Go cue") in the catch trials.

Figure 5a shows topographical plots of group-averaged ERD/S in the β -frequency band. Whole EEG channel-averaged ERD in the β -frequency band is plotted in Figure 5b. Using the linear mixed effects modeling, we found a significant main effect of FORCE LEVEL ($F_{[2,\ 587]}=6.05, p=.002$). Post hoc follow-up tests showed that ERD in the β -frequency band in the 25% MVC condition was significantly enhanced compared to that in the 5% MVC condition (p=.003) and

FIGURE 3 Effect of β-rhTMS on zPLF in β frequency. (a) Groupaveraged time-frequency representation of zPLF across significant EEG channels identified at the 25% MVC condition. Green dotted lines denote the frequency band and time window used for averaging zPLF values for each force condition. (b) Topographical plots of group-averaged zPLF in the β-frequency band. Based on cluster-based comparisons. t statistical map was shown at the right column using red-blue scale and significant channels between β-rhTMS and sham are overlaid as red dots (cluster-threshold: p < .05). Higher synchronous EEG oscillations in the β-frequency band were distributed across the contra- and ipsilateral sensorimotor areas and especially for the 25% MVC condition (bottom row).





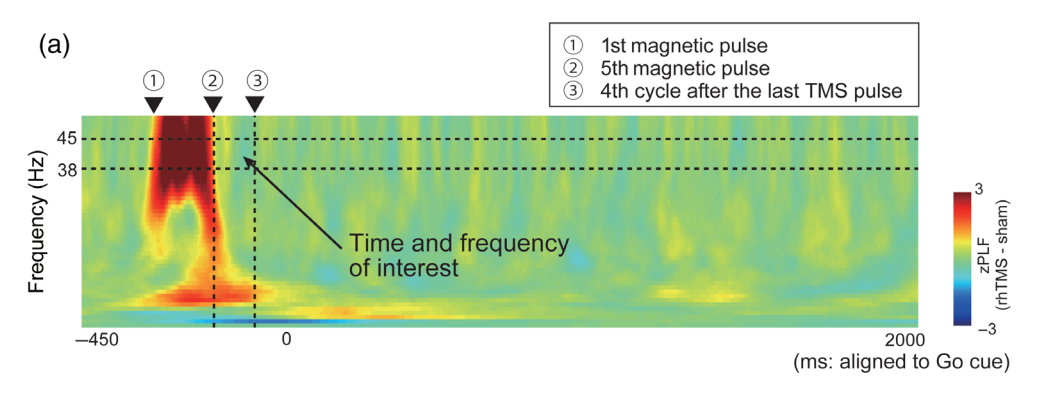
the comparison between 25% and 10% MVC conditions was close to statistical significance (p=.07). These results indicate that EEG power (ERD) decreased as the magnitude of force output increased. Therefore, for greater force outputs, rhTMS-induced EEG entrainments were more likely to occur when the EEG oscillations are dominated by ERD.

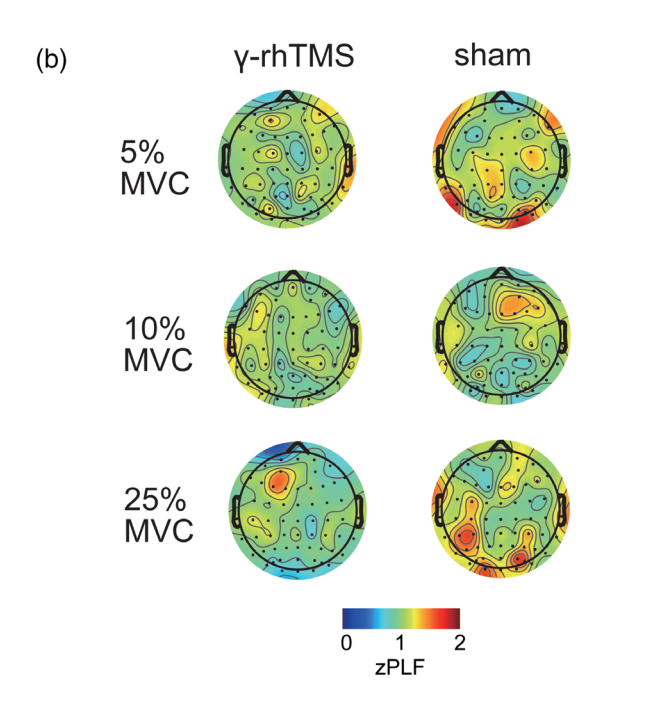
3.3 | Experiment 2: Arrhythmic TMS

Experiment 1 demonstrated that $\beta\text{-rhTMS}$ elicited significantly slowed peak force rate for the 25% MVC condition whereas $\gamma\text{-rhTMS}$ had no effect on behavior. This observation supports the premise that rhTMS can exert phasic effects at the targeted β oscillation. However, previous studies raise several concerns about the validity of effects of rhTMS on neural and behavioral changes. Specifically, rhTMS could have only induced a phase-resetting effect that is neither rhythmic nor frequency specific. If so, arrhythmic TMS (arTMS) would change zPLF and peak force rate in the same way as rhTMS did. To address

this question, we delivered arTMS at β - and γ -frequencies as an additional control condition (Figure 1b).

Figure 6a shows changes in zPLF values across the two arTMS conditions and catch trials. Note that the protocol in Experiment 2 did not include β - and γ -rhTMS under the 10% MVC condition and all sham conditions due to the constraints on the maximum total duration of data collection since we used a within-subject design here. Based on the cluster-based comparisons, there were no significant differences in zPLF between arTMS and catch conditions across the two force levels (p > .05 each). Figure 6b shows changes in peak force rate across the two arTMS conditions. The mixed-effect model revealed a significant main effect of FORCE LEVEL ($F_{1, 117, 160} = 1118.66, p = 2$ imes 10⁻¹⁶) and no significant main effect of STIMULATION TYPE (F₂, $_{392} = 1.87, p = .15$) or interaction ($F_{2,302} = 1.44, p = .23$). The lack of significant differences in peak force rate across stimulation types (βand y-arrhythmic TMS versus catch) supports the interpretation of our findings from Experiment 1: the periodicity of external inputs (i.e., rhythmic magnetic pulses) is essential for the manipulation of motor behavior.





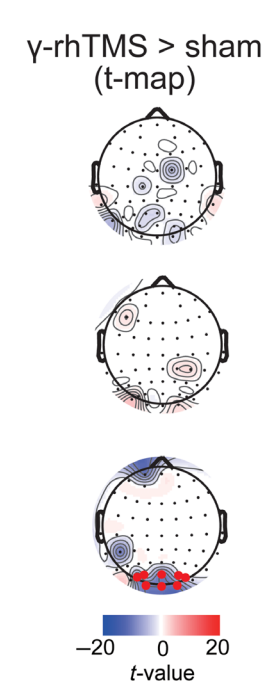


FIGURE 4 Effect of γ-rhTMS on zPLF on γ -frequency. (a) Group-averaged timefrequency representation of zPLF at C3 channel in the 25% MVC condition. Dot lines denote the frequency band and time window used for averaging zPLF values were averaged for each force condition. (b) Topographical plots of group-averaged zPLF in the v-frequency band (38-45 Hz). Based on cluster-based comparisons, t statistical map was shown at the right column using red-blue scale and significant channels between y-rhTMS and sham are overlaid as red dots (cluster-threshold: p < .05). Lower synchronous EEG oscillations in the γ-frequency band were identified in the 25% MVC than sham condition (b. bottom row).

4 | DISCUSSION

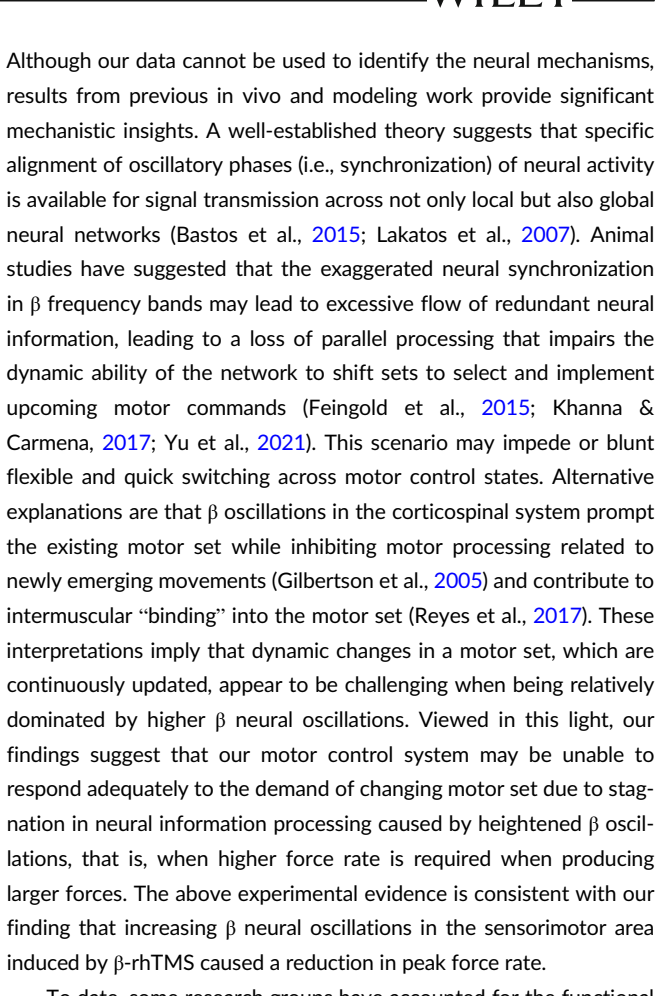
By combining rhTMS, EEG and behavioral measures, we sought to determine whether M1 β neural oscillations are associated with motor vigor. β -rhTMS in Experiment 1 caused modulation of β neural oscillations in the sensorimotor area coinciding with the reduction of peak force rate only for the high force level (25% MVC).

As expected, γ -rhTMS failed to entrain γ neural oscillations or peak force rate. In Experiment 2 we used β - and γ -arTMS to determine whether the above neural and behavioral effects were merely the result of nonrhythmic single pulses, which can induce phase-resetting. Both of these stimulation modalities failed to induce modulation of neural and behavioral responses. Furthermore, we found that β ERD (less synchronization) significantly increased for the 25% MVC condition (high level of motor vigor) relative to the 5% and 10% MVC conditions. This indicates that the effect of β -rhTMS on cortical oscillations occurred primarily when neural oscillations were less synchronized, leading to the reduction of peak force rate. A recent study reported that β -rhTMS can drive neural oscillations in the human corticospinal system to the β frequency during a resting state, but there

was no evidence whether the effect of rhTMS may spill over to voluntary movements (Romei, Bauer, et al., 2016). Here, for the first time we demonstrate that $\beta\text{-rhTMS}$ leads to a reduction in the vigor of motor responses in parallel with a modulation of β cortical oscillations. Importantly, this effect appears to be dependent on the magnitude of motor output vigor, this scenario being associated with the highest level of neural oscillation desynchronization.

4.1 | Role of β neural oscillations for motor vigor

 β neural oscillations are inextricably associated with motor control (Barone & Rossiter, 2021). It has been reported that increased subthalamic nucleus (STN) β power (William et al., 2005) and STN coherence with M1 (van Wijk et al., 2017) correlate with longer reaction times. In a Go/Nogo task, changes in β power only emerged in the frontal and sensorimotor areas for successful stop performance (Swann et al., 2009). Regarding the pathophysiological feature of β neural oscillations, this oscillation was strongly enhanced in Parkinson's disease throughout the cortico-basal ganglia-thalamic loop and strongly



To date, some research groups have accounted for the functional role of β neural oscillations in motor vigor by using noninvasive brain stimulation delivered by tACS (Joundi, Jenkinson, et al., 2012; Moisa et al., 2016), but there was little consensus regarding the relation between β oscillations and motor vigor. However, the results of these previous studies are difficult to interpret because they did not monitor ongoing neural activity using EEG. Therefore, it cannot be established when β neural oscillations induced by tACS emerged relative to motor

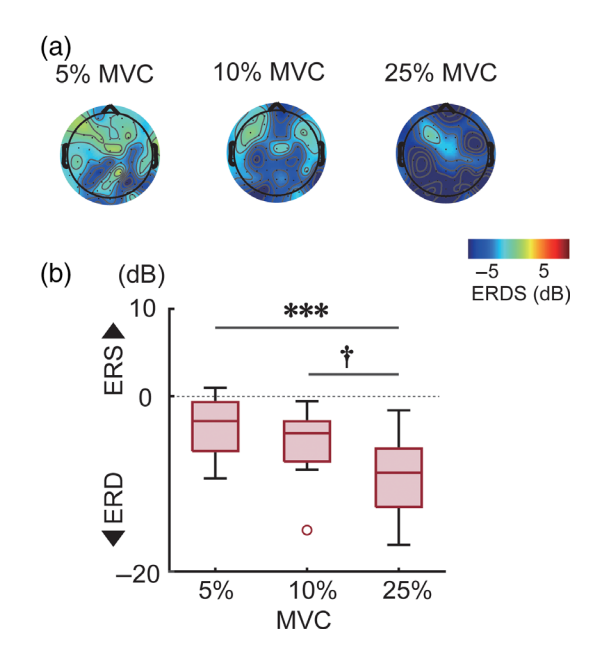


FIGURE 5 Baseline EEG power changes (catch trial) in each force level. (a) Topographical plots of group-averaged EEG power in the β -frequency band (-300 to -50 ms relative to "Go cue": Same time window as rhTMS) that were obtained from the catch trials. (b) Whole channel averaged EEG powers in the β frequency band across the force level. *** and \dagger depict p < .001 and .07, respectively.

correlated with their symptoms, for example, bradykinesia (slowness of movement) and rigidity (Little & Brown, 2014).

The neurophysiological role of β neural oscillations in motor vigor is still a matter of debate (Barone & Rossiter, 2021; Engel & Fries, 2010; Khanna & Carmena, 2017; Moisa et al., 2016; Torrecillos et al., 2018). In the present study, driving β cortical oscillations by using rhTMS led to a decrease in peak force rate and this effect was stronger when a high level of motor vigor was required, indicating that β neural oscillations are necessary for the modulation of motor vigor.

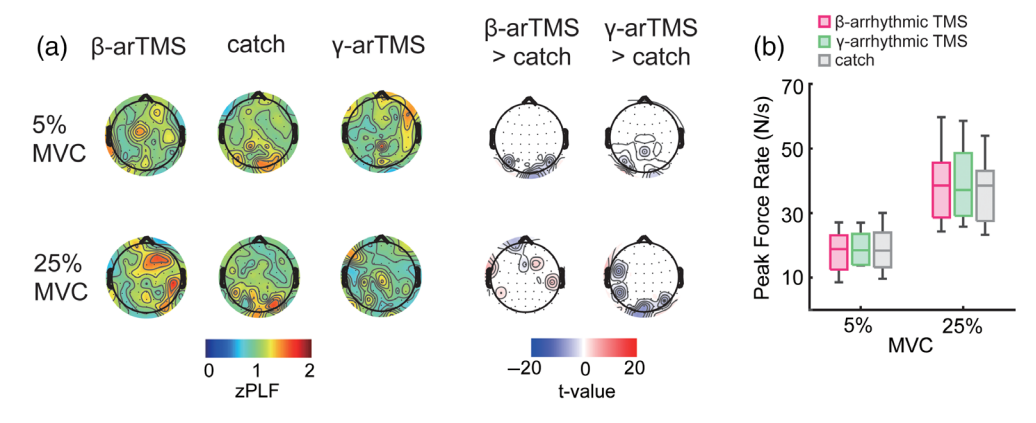


FIGURE 6 EEG and behavioral results of the arTMS condition. (a) Effects of arTMS on the zPLF changes. Using cluster-based comparisons, statistical t-map is illustrated at the middle of this figure. (b) Effects of arTMS on peak force rate. Boxplots depict median (crossbar) and minimum and maximum values (whiskers). Boxplots visualizing group-averaged peak force rate in each condition. The mixed effect linear model yielded no significant differences in peak force rate across the stimulus condition within the both MVC condition.

10970193, 2023, 3, Downloaded from https://onlinelibrary.wiley.com/doi/10.1002/hbm.26149, Wiley Online Library on [25/01/2023]. See the Terms and Conditions (https://onlinelibrary.wiley.com/terms-and-conditions) on Wiley Online Library for rules of use; OA articles are governed by the applicable Creative Commons. Licensee

execution, such as during motor preparation or shortly after movement onset. Moreover, previous work did not deliver tACS in an event-related manner and stimulus intensity was not individualized based on a specific assessment of cortical excitability. Such a fixeddose (i.e., "one-size-fits-all") approach likely results in substantial interindividual variability (Li et al., 2015). An additional limitation of tACS studies is that tACS has lower degree of spatial resolution than TMS. In the present study, our rhTMS protocol addressed these methodological issues. Specifically, we adjusted TMS intensity to each subject by assessing individual motor-evoked potentials and by focally stimulating a small cortical area (1-2 cm²) through a figure-of-eight coil (Fertonani & Miniussi, 2017; Ridding & Rothwell, 2007).

In this light of these methodological considerations, our EEGrhTMS protocol provides novel evidence that β neural oscillations in the sensorimotor area play an inhibitory role on motor vigor. Our findings are an important first step toward disentangling the complex relation between oscillatory neural dynamics and motor behavior, while corroborating existing evidence obtained through a correlative approach.

The effect of β-rhTMS was sensitive to 4.2 required force level

One of our main findings is that the effect of β-rhTMS on motor responses was sensitive to force level as β-rhTMS reduced peak force rate only for the 25% MVC condition. As shown in Figure 2, it was confirmed that the peak force rate was also higher as the level of the force production increased. Thus, the high level of force production (25% MVC) required greater motor vigor. Indeed, we had initially hypothesized that the suppression of motor vigor induced by β cortical oscillations depended on the magnitude of peak force rate. However, the present study went a step further and revealed that EEG power changes provide a clue to understanding this phenomenon: EEG power was significantly lower for higher force levels, as indicated by ERD immediately before the onset of force production. ERD and ERS have been used to quantify the dynamics of neural activity that implies frequency-specific changes of ongoing EEG activity (Pfurtscheller, 1992). By combining our EEG entrainment (i.e., zPLF) with EEG power changes, rhTMS-induced EEG entrainment was more likely to occur when the EEG oscillations are dominated by ERD. A previous computational model study demonstrated that the mechanism by which periodic brain stimulation (i.e., rhTMS) affects ongoing brain activity depends on the brain state, for example, resting versus engaged. For example, a state of ERD is more prone to an entrainment of ongoing EEG activity during or after periodic brain stimulation than ERS (Alagapan et al., 2016). More recently, an animal study combining noninvasive brain stimulation and local field potentials also suggested that a dynamic interplay of ongoing neural oscillations and brain stimulation depends on brain states (Krause et al., 2022). A state of ERS implies that synchronized neural oscillations is robust and has tightly stabilized in an oscillatory attractor. That is, a state of neural oscillation in β frequency being already in an in-phase pattern hampered

rhTMS effects due to possible ceiling effects. Therefore, the finding that rhTMS affected motor vigor only for the 25% MVC condition can be explained by the fact that the 5% and 10% MVC conditions tended to be dominated by more ERS than ERD relatively to the 25% MVC condition. Together, our findings highlight that ongoing brain states can impact response to rhTMS.

4.3 Optimal frequency for the neural entrainments in M1

 β -rhTMS was able to successfully entrain β neural oscillations around the sensorimotor area and its entrainment lasted for a few cycles immediately after the 5th magnetic pulse (last pulse of rhTMS), but γ-rhTMS did not. This observation may be due to the fact that different brain regions engage in neural oscillations at different frequencies. For instance, even though spontaneous neural oscillations recorded by E/MEG are rather variable, occipital areas typically oscillate at α rhythm (Hillebrand et al., 2012; Omata et al., 2013; Romei et al., 2010; Romei, Rihs, et al., 2008), whereas \sim 20 Hz rhythms(β frequency) emerge around the sensorimotor area (Bai et al., 2008: Brookes et al., 2011: Gilbertson et al., 2005: Hipp et al., 2012). Thus, each cortical area appears to be characterized by a specific neural oscillation frequency which is thought to spatially organize the activity of neural ensembles. This is plausible because a TMS-EEG study showing that, α , β and β/γ rhythms emerged at the occipital, parietal and frontal cortices, respectively (Rosanova et al., 2009). More direct evidence is that Okazaki et al. (2021) also replicated this by using the combination of rhTMS with the EEG recording. Thus, each brain area may preserve its own natural frequency and rhTMS manipulate oscillations close to natural frequency. In line with converging evidence, we found that β-rhTMS was able to entrain neural oscillations predominantly in the β -frequency band, whereas low γ -rhTMS (40 Hz) did not as this neural oscillation frequency does not naturally occur in the sensorimotor area. Therefore, low γ rhythms induced by γ -rhTMS reverted to the natural frequency immediately after the stimulation.

STUDY LIMITATIONS

First, although several rhTMS-EEG studies used stimulus frequencies adjusted to each subject's alpha- (Di Gregorio et al., 2022; Thut, Veniero, et al., 2011) or beta-peak frequency (Romei, Bauer, et al., 2016), we chose to use fixed stimulus frequencies. This choice was motivated by time constraints and the possible occurrence of mental fatigue in our participants. Specifically, measuring individual beta- or gamma-frequencies prior to performing all of our experimental and control conditions would have significantly lengthened the duration of the experimental session. However, we acknowledge that using a fixed rhTMS frequency may be suboptimal in maximizing the entrainment effects on neural oscillations, as indicated by a previous study (Romei, Bauer, et al., 2016). The study by Romei and colleagues

UEHARA ET AL. WILEY 1169

reported that changes in neural oscillations significantly differed between individual beta-peak frequency (IBF) and surrounding IBF, even though rhTMS at surrounding IBF (±6 Hz) also successfully entrained the target neural oscillations relative to sham stimulation. Therefore, it is possible that rhTMS delivered at individualized frequencies could have potentially affected peak-force rate at the lower MVC condition.

Second, Experiment 1 (β -rhTMS and γ -rhTMS) and Experiment 2 (arTMS) are characterized by different groups and numbers of subjects, as well as MVC conditions (for the β -rhTMS and γ -rhTMS we tested three MVC conditions, whereas for the arTMS we tested two MVC conditions). We chose not to test the sham condition and 10% MVC condition in Experiment 2 to minimize the risk of subjects' cognitive and physical fatigue. We believe our approach is justified for two additional reasons: (1) behavioral and EEG results from the sham condition did not differ from those in the catch condition and (2) βand γ-rhTMS did not affect peak force rate changes in the 10% MVC condition. Although lack of the sham and 10% MVC conditions in Experiment 2 is a limitation of the present study, we believe it would not impact the interpretation of our experimental results. Additionally, Experiment 1 and Experiment 2 were conducted on different groups of subjects. A second limitation is that is the potential confounding factor of interindividual variability of the stimulus effects (Li et al., 2015). These limitations must be considered when interpreting our results.

5.1 | Future directions

We suggest some future directions in our work. First, in this study rhTMS was time-locked to an epoch immediately before the force production across all trials to simplify our data collection. However, dynamics of neural oscillations involved in motor and cognitive behaviors may flexibly differ across trials due to latent brain states (i.e., trial-by-trial latent variabilities) (Arazi & IIan, 2017; Fox et al., 2006). Therefore, our next step will be to develop a closed-loop rhTMS system that combines modulating brain stimulation with measuring of ongoing neural oscillations. Recently, a brain state-informed stimulation with real-time estimation of EEG oscillations using the Kalman filter or autoregressive model was proposed (Onojima & Kitajo, 2021; Shakeel et al., 2021; Zrenner et al., 2018). These novel approaches would help us to gain new insights into how M1 β oscillations contribute to motor behavior.

Second, our study shows the potential of modulating neural oscillations together with behavioral response. This observation points to potential clinical applications, for example, diagnosis or treatment of movement disorders, which arise from abnormalities in neural oscillations. Although this has not yet proven to be an effective approach in patients affected by Parkinson's disease and dystonia (Georgescu et al., 2018; Hess et al., 2020; Little & Brown, 2014), rhTMS could be considered as a promising new therapeutic tool to modulate specific neural oscillations in the sensorimotor cortex.

6 | CONCLUSIONS

We show here, for the first time, that β -rhTMS delivered to the human sensorimotor area modulated neural oscillations in the β frequency and that this modulation was associated with a reduction of motor vigor (i.e., peak force rate), as shown by earlier correlation approaches. Although further work is needed, our data supports the notion that beta cortical oscillations in M1 plays an important role in the regulation of motor vigor. Another key finding of the present study is that the neural and behavioral effects of rhTMS depend on the state of cortical oscillations: the greatest effect occurs when neural oscillations are characterized by an out-of-phase pattern, that is, desynchronization. Our findings have significant potential for the design of new research and therapeutic noninvasive brain stimulation protocols to address sensorimotor and cognitive pathologies characterized by dysfunctional patterns of neural oscillation dynamics.

AUTHOR CONTRIBUTIONS

Kazumasa Uehara, Justin M. Fine, and Marco Santello designed experiment; Kazumasa Uehara performed data collection; Kazumasa Uehara and Justin M. Fine analyzed data; Kazumasa Uehara, Justin M. Fine, and Marco Santello wrote the article.

ACKNOWLEDGMENTS

We thank Mr. Akihiko Ishihara, Mr. Minh Pham, and Ms. Romann Arizmendi for their assistance with data collection. This study was supported by a National Science Foundation grant (BCS-1827752).

DATA AVAILABILITY STATEMENT

The data that support the findings in this study are available from the corresponding author upon reasonable request.

ORCID

Kazumasa Uehara https://orcid.org/0000-0003-2350-8694

REFERENCES

Alagapan, S., Schmidt, S. L., Lefebvre, J., Hadar, E., Shin, H. W., & Fröhlich, F. (2016). Modulation of cortical oscillations by low-frequency direct cortical stimulation is state-dependent. *PLoS Biology*, 14, 1–21.

Albouy, P., Weiss, A., Baillet, S., & Zatorre, R. J. (2017). Selective entrainment of theta oscillations in the dorsal stream causally enhances auditory working memory performance. *Neuron*, *94*, 193–206.

Androulidakis, A. G., Doyle, L. M. F., Gilbertson, T. P., & Brown, P. (2006). Corrective movements in response to displacements in visual feedback are more effective during periods of 13–35 Hz oscillatory synchrony in the human corticospinal system. *The European Journal of Neuroscience*, 24, 3299–3304.

Androulidakis, A. G., Doyle, L. M. F., Yarrow, K., Litvak, V., Gilbertson, T. P., & Brown, P. (2007). Anticipatory changes in beta synchrony in the human corticospinal system and associated improvements in task performance. The European Journal of Neuroscience, 25, 3758–3765.

Arazi, A., G. G.-Y., & Ilan, D. (2017). The magnitude of trial-by-trial neural variability is reproducible over time and across tasks in humans. *eNeuro*, 4, 1–12.

- Bai, O., Lin, P., Vorbach, S., Floeter, M. K., Hattori, N., & Hallett, M. (2008). A high performance sensorimotor beta rhythm-based brain-computer interface associated with human natural motor behavior. *Journal of Neural Engineering*, 5, 24–35.
- Ball, T., Demandt, E., Mutschler, I., Neitzel, E., Mehring, C., Vogt, K., Aertsen, A., & Schulze-Bonhage, A. (2008). Movement related activity in the high gamma range of the human EEG. *NeuroImage*, 41, 302–310.
- Barone, J., & Rossiter, H. E. (2021). Understanding the role of sensorimotor Beta oscillations. Frontiers in Systems Neuroscience, 15, 1–7.
- Bastos, A. M., Vezoli, J., & Fries, P. (2015). Communication through coherence with inter-areal delays. *Current Opinion in Neurobiology*, 31, 173–180.
- Bjorg, K., Zaepffel, M., Brovelli, A., Mackay, W., & Riehle, A. (2013). The ups and downs of beta oscillations in sensorimotor cortex. *Experimental Neurology*, 245, 15–26.
- Brittain, J. S., & Brown, P. (2014). Oscillations and the basal ganglia: Motor control and beyond. *NeuroImage*, 85, 637–647.
- Brookes, M. J., Hale, J. R., Zumer, J. M., Stevenson, C. M., Francis, S. T., Barnes, G. R., Owen, J. P., Morris, P. G., & Nagarajan, S. S. (2011). Measuring functional connectivity using MEG: Methodology and comparison with fcMRI. *NeuroImage*, 56, 1082–1104.
- Brown, P. (2000). Cortical drives to human muscle: The piper and related rhythms. *Progress in Neurobiology*, *60*, 97–108.
- Brucke, C., Huebl, J., Schonecker, T., Neumann, W.-J., Yarrow, K., Kupsch, A., Blahak, C., Lutjens, G., Brown, P., Krauss, J. K., Schneider, G.-H., & Kuhn, A. A. (2012). Scaling of movement is related to Pallidal oscillations in patients with dystonia. *The Journal of Neuroscience*, 32, 1008–1019.
- Buzsáki, G., & Draguhn, A. (2004). Neuronal oscillations in cortical networks. *Science*, 304, 1926–1929.
- Chanes, L., Quentin, R., Tallon-Baudry, C., & Valero-Cabré, A. (2013). Causal frequency-specific contributions of frontal spatiotemporal patterns induced by non-invasive neurostimulation to human visual performance. The Journal of Neuroscience, 33, 5000–5005.
- Cheyne, D., Bells, S., Ferrari, P., Gaetz, W., & Bostan, A. C. (2008). Self-paced movements induce high-frequency gamma oscillations in primary motor cortex. *NeuroImage*, 42, 332–342.
- Cheyne, D., & Ferrari, P. (2013). MEG studies of motor cortex gamma oscillations: Evidence for a gamma "fingerprint" in the brain? Frontiers in Human Neuroscience, 7, 1–7.
- Chipchase, L. S., Schabrun, S. M., & Hodges, P. W. (2011). Peripheral electrical stimulation to induce cortical plasticity: A systematic review of stimulus parameters. Clinical Neurophysiology, 122, 456-463.
- Chen, C. C., Vladimir, L., Thomas, G., Andrea, K., Chin, S. L., Shih, T. L., Chon, H. T., Stephen, T., Patricia, L., Marwan, H., & Peter, B. (2007) Excessive synchronization of basal ganglia neurons at 20 Hz slows movement in Parkinson's disease. *Experimental Neurology* 205, 214–221.
- David, W., Andrea, K., Andreas, K., Marina, T., Gerard van Bruggen, Hans, S., Gary, H., Constantinos, L., & Peter, B. (2005). The relationship between oscillatory activity and motor reaction time in the parkinsonian subthalamic nucleus. The European journal of neuroscience. 21, 249–258.
- Delorme, A., & Makeig, S. (2004). EEGLAB: An open source toolbox for analysis of single-trial EEG dynamics including independent component analysis. *Journal of Neuroscience Methods*, 134, 9–21.
- Di Gregorio, F., Trajkovic, J., Roperti, C., Marcantoni, E., Di Luzio, P., Avenanti, A., Thut, G., & Romei, V. (2022). Tuning alpha rhythms to shape conscious visual perception. *Current Biology*, *32*, 988–998.e6.
- Engel, A. K., & Fries, P. (2010). Beta-band oscillations-signalling the status quo? *Current Opinion in Neurobiology*, 20, 156–165.
- Feingold, J., Gibson, D. J., Depasquale, B., & Graybiel, A. M. (2015). Bursts of beta oscillation differentiate postperformance activity in the striatum and motor cortex of monkeys performing movement tasks.

- Proceedings of the National Academy of Sciences of the United States of America, 112, 13687–13692.
- Fertonani, A., & Miniussi, C. (2017). Transcranial electrical stimulation: What we know and do not know about mechanisms. *The Neuroscientist*, 23, 109–123.
- Fisher, N. I. (1995). Statistical analysis of circular Datatle. Cambridge University Press.
- Fox, M. D., Snyder, A. Z., Zacks, J. M., & Raichle, M. E. (2006). Coherent spontaneous activity accounts for trial-to-trial variability in human evoked brain responses. *Nature Neuroscience*, *9*, 23–25.
- Farzan, F., Vernet, M., Shafi, M. M. D., Rotenberg, A., Daskalakis, Z. J., & Pascual-Leone, A. (2016). Characterizing and modulating brain circuitry through transcranial magnetic stimulation combined with electroencephalography. Frontiers in Neural Circuits, 10(73), 1–24.
- Georgescu, E. L., Georgescu, I. A., Zahiu, C. D. M., Şteopoaie, A. R., Morozan, V. P., Pană, A. Ş., Zăgrean, A. M., & Popa, D. (2018). Oscillatory cortical activity in an animal model of dystonia caused by cerebellar dysfunction. Frontiers in Cellular Neuroscience, 12, 1–23.
- Gilbertson, T., Lalo, E., Doyle, L., Di Lazzaro, V., Cioni, B., & Peter, B. (2005). Existing motor state is favored at the expense of new movement during 13–35 Hz oscillatory synchrony in the human corticospinal system. *The Journal of Neuroscience*, 25, 7771–7779.
- Hess, C. W., Gatto, B., Chung, J. W., Ho, R. L. M., Wang, W., Wagle Shukla, A., & Vaillancourt, D. E. (2020). Cortical oscillations in cervical dystonia and dystonic tremor. Cerebral Cortex Communications, 1, 1–13.
- Hillebrand, A., Barnes, G. R., Bosboom, J. L., Berendse, H. W., & Stam, C. J. (2012). Frequency-dependent functional connectivity within restingstate networks: An atlas-based MEG beamformer solution. *Neuro-Image*, 59, 3909–3921.
- Hipp, J. F., Hawellek, D. J., Corbetta, M., Siegel, M., & Engel, A. K. (2012). Large-scale cortical correlation structure of spontaneous oscillatory activity. *Nature Neuroscience*, 15, 884–890.
- Joundi, R. A., Brittain, J. S., Green, A. L., Aziz, T. Z., Brown, P., & Jenkinson, N. (2012). Oscillatory activity in the subthalamic nucleus during arm reaching in Parkinson's disease. *Experimental Neurology*, 236, 319–326.
- Joundi, R. A., Jenkinson, N., Brittain, J.-S., Aziz, T. Z., & Brown, P. (2012). Driving oscillatory activity in the human cortex enhances motor performance. *Current Biology*, 22, 403–407.
- Kawasaki, M., Uno, Y., Mori, J., Kobata, K., & Kitajo, K. (2014). Transcranial magnetic stimulation-induced global propagation of transient phase resetting associated with directional information flow. Frontiers in Human Neuroscience, 8, 173.
- Kayser, J., & Tenke, C. E. (2006). Principal components analysis of Laplacian waveforms as a generic method for identifying ERP generator patterns: II. Adequacy of low-density estimates. Clinical Neurophysiology, 117, 369–380.
- Keel, J. C., Smith, M. J., & Wassermann, E. M. (2000). A safety screening questionnaire for transcranial magnetic stimulation. *Clinical Neurophysiology*, 112, 720.
- Khanna, P., & Carmena, J. M. (2017). Beta band oscillations in motor cortex reflect neural population signals that delay movement onset. *eLife*, 6, e24573
- Krause, M. R., Vieira, P. G., Thivierge, J.-P., & Pack, C. C. (2022). Brain stimulation competes with ongoing oscillations for control of spike timing in the primate brain. *PLoS Biology*, 20, e3001650.
- Krueger, C. (2004). A comparison of the general linear mixed model and repeated measures ANOVA using a dataset with multiple missing data points. *Biological Research for Nursing*, *6*, 151–157.
- Kuznetsova, A., Brockhoff, P., & Christensen, R. (2016). ImerTest: Tests in linear mixed effects models. R Packag version 3.0.0. https://cran.rproject.org/package=ImerTest
- Lachaux, J.-P., Rodriguez, E., M LVQ, A L, J M, & Varela, F. J. (2000). Studying signale-trials of phase synchronous activity in the brain. *International Journal of Bifurcationand Chaos*, 10, 2429–2439.

UEHARA ET AL. WILEY 1171

- Lakatos, P., Chen, C. M., O'Connell, M. N., Mills, A., & Schroeder, C. E. (2007). Neuronal oscillations and multisensory interaction in primary auditory cortex. *Neuron*, 53, 279–292.
- Li, L. M., Uehara, K., & Hanakawa, T. (2015). The contribution of interindividual factors to variability of response in transcranial direct current stimulation studies. *Frontiers in Cellular Neuroscience*, *9*, 181.
- Lin, Y. J., Shukla, L., Dugué, L., Valero-Cabré, A., & Carrasco, M. (2021). Transcranial magnetic stimulation entrains alpha oscillatory activity in occipital cortex. Scientific Reports, 11, 1–14.
- Little, S., & Brown, P. (2014). The functional role of beta oscillations in Parkinson's disease. *Parkinsonism & Related Disorders*, 20, S44–S48.
- Maris, E., & Oostenveld, R. (2007). Nonparametric statistical testing of EEG- and MEG-data. *Journal of Neuroscience Methods*, 164, 177-190.
- Mazaheri, A., & Jensen, O. (2006). Posterior activity is not phase-reset by visual stimuli. Proceedings of the National Academy of Sciences, 103, 2948–2952.
- Mima, T., Simpkins, N., Oluwatimilehin, T., & Hallett, M. (1999). Force level modulates human cortical oscillatory activities. *Neuroscience Letters*, 275, 77–80.
- Moisa, M., Polania, R., Grueschow, M., & Ruff, C. C. (2016). Brain network mechanisms underlying motor enhancement by transcranial entrainment of gamma oscillations. *The Journal of Neuroscience*, 36, 12053– 12065.
- Muthukumaraswamy, S. D. (2010). Functional properties of human primary motor cortex gamma oscillations. *Journal of Neurophysiology*, 104. 2873–2885.
- Nikouline, V., Ruohonen, J., & Ilmoniemi, R. J. (1999). The role of the coil click in TMS assessed with simultaneous EEG. Clinical Neurophysiology, 110, 1325–1328.
- Okazaki, Y. O., Nakagawa, Y., Mizuno, Y., Hanakawa, T., & Kitajo, K. (2021). Frequency- and area-specific phase entrainment of intrinsic cortical oscillations by repetitive transcranial magnetic stimulation. Frontiers in Human Neuroscience, 15, 1–13.
- Omata, K., Hanakawa, T., Morimoto, M., & Honda, M. (2013). Spontaneous slow fluctuation of EEG alpha rhythm reflects activity in deep-brain structures: A simultaneous EEG-fMRI study. *PLoS One*, 8, 1–12.
- Onojima, T., & Kitajo, K. (2021). A state-informed stimulation approach with real-time estimation of the instantaneous phase of neural oscillations by a Kalman filter. *Journal of Neural Engineering*, 18, 066001.
- Perrin, F., Pernier, J., Bertrand, O., & Echallier, J. F. (1989). Spherical splines for scalp potential and current density mapping. *Electroencephalogra*phy and Clinical Neurophysiology, 72, 184–187.
- Pfurtscheller, G. (1992). Event-related synchronization (ERS): An electrophysiological correlate of cortical areas at rest. *Electroencephalography* and Clinical Neurophysiology, 83, 62–69.
- Pfurtscheller, G., & Lopes Da Silva, F. H. (1999). Event-related EEG/MEG synchronization and desynchronization: Basic principles. Clinical Neurophysiology, 110, 1842–1857.
- Pinheiro, J., Bates, D., DebRoy, S., Sarkar, D., & Team, R. C. (2017). *nlme:* Linear and nonlinear mixed effects models. R package version 3.1-131. https://CRAN.R-project.org/package¹/4nlme
- Pogosyan, A., Gaynor, L. D., Eusebio, A., & Brown, P. (2009). Boosting cortical activity at Beta-band frequencies slows movement in humans. Current Biology, 19, 1637–1641.
- Radüntz, T., Scouten, J., Hochmuth, O., & Meffert, B. (2015). EEG artifact elimination by extraction of ICA-component features using image processing algorithms. *Journal of Neuroscience Methods*, 243, 84–93.
- Reyes, A., Laine, C. M., Kutch, J. J., & Valero-Cuevas, F. J. (2017). Beta band Corticomuscular drive reflects muscle coordination strategies. Frontiers in Computational Neuroscience, 11, 1–10.
- Ridding, M. C., & Rothwell, J. C. (2007). Is there a future for therapeutic use of transcranial magnetic stimulation? *Nature Reviews. Neuroscience*, 8, 559–567.

- Romei, V., Bauer, M., Brooks, J. L., Economides, M., Penny, W., Thut, G., Driver, J., & Bestmann, S. (2016). Causal evidence that intrinsic betafrequency is relevant for enhanced signal propagation in the motor system as shown through rhythmic TMS. *NeuroImage*, 126, 120–130.
- Romei, V., Gross, J., & Thut, G. (2010). On the role of prestimulus alpha rhythms over occipito-parietal areas in visual input regulation: Correlation or causation? *The Journal of Neuroscience*, 30, 8692–8697.
- Romei, V., Rihs, T., Brodbeck, V., & Thut, G. (2008). Resting electroencephalogram alpha-power over posterior sites indexes baseline visual cortex excitability. *Neuroreport*, 19, 203–208.
- Romei, V., Thut, G., & Silvanto, J. (2016). Information-based approaches of noninvasive transcranial brain stimulation. *Trends in Neurosciences*, 39, 782–795.
- Romero, S., Mañanas, M. A., & Barbanoj, M. J. (2008). A comparative study of automatic techniques for ocular artifact reduction in spontaneous EEG signals based on clinical target variables: A simulation case. Computers in Biology and Medicine, 38, 348–360.
- Rosanova, M., Casali, A. G., Bellina, V., Resta, F., Mariotti, M., & Massimini, M. (2009). Natural frequencies of human Corticothalamic circuits. *The Journal of Neuroscience*, 29, 7679–7685.
- Rossi, S., Hallett, M., Rossini, P. M., & Pascual-Leone, A. (2009). Safety, ethical considerations, and application guidelines for the use of transcranial magnetic stimulation in clinical practice and research. *Clinical Neurophysiology*, 120, 2008–2039.
- Salenius, S., Salmelin, R., Neuper, C., Pfurtscheller, G., & Hari, R. (1996).
 Human cortical 40 Hz rhythm is closely related to EMG rhythmicity.
 Neuroscience Letters, 213, 75–78.
- Santarnecchi, E., Biasella, A., Tatti, E., Rossi, A., Prattichizzo, D., & Rossi, S. (2017). High-gamma oscillations in the motor cortex during visuomotor coordination: A tACS interferential study. *Brain Research Bulle*tin. 131, 47–54.
- Shakeel, A., Onojima, T., Tanaka, T., & Kitajo, K. (2021). Real-time implementation of eeg oscillatory phase-informed visual stimulation using a least mean square-based ar model. *Journal of Personalized Medicine*, 11, 1–16.
- Swann, N., Tandon, N., Canolty, R., Ellmore, T. M., McEvoy, L. K., Dreyer, S., DiSano, M., & Aron, A. R. (2009). Intracranial EEG reveals a time- and frequency-specific role for the right inferior frontal gyrus and primary motor cortex in stopping initiated responses. *The Journal* of Neuroscience, 29, 12675–12685.
- Tallon-Baudry, C., Bertrand, O., Delpuech, C., & Pernier, J. (1996). Stimulus specificity of phase-locked and non-phase-locked 40 Hz visual responses in human. The Journal of Neuroscience, 16, 4240–4249.
- Tan, H., Pogosyan, A., Ashkan, K., Cheeran, B., FitzGerald, J. J., Green, A. L., Aziz, T., Foltynie, T., Limousin, P., Zrinzo, L., & Brown, P. (2015). Subthalamic nucleus local field potential activity helps encode motor effort rather than force in parkinsonism. The Journal of Neuroscience, 35, 5941–5949.
- Thut, G. (2014). Modulating brain oscillations to drive brain function. PLoS Biology, 12, 1–4.
- Thut, G., Schyns, P. G., & Gross, J. (2011). Entrainment of perceptually relevant brain oscillations by non-invasive rhythmic stimulation of the human brain. *Frontiers in Psychology*, 2, 1–10.
- Thut, G., Veniero, D., Romei, V., Miniussi, C., Schyns, P., & Gross, J. (2011).
 Rhythmic TMS causes local entrainment of natural oscillatory signatures. *Current Biology*, 21, 1176–1185.
- Torrecillos, F., Tinkhauser, G., Fischer, P., Green, A. L., Aziz, T. Z., Foltynie, T., Limousin, P., Zrinzo, L., Ashkan, K., Brown, P., & Tan, H. (2018). Modulation of beta bursts in the subthalamic nucleus predicts motor performance. *The Journal of Neuroscience*, 38, 8905–8917.
- Trajkovic, J., Di Gregorio, F., Marcantoni, E., Thut, G., & Romei, V. (2022). A TMS/EEG protocol for the causal assessment of the functions of the oscillatory brain rhythms in perceptual and cognitive processes. STAR Protocols, 3, 101435.
- Tzagarakis, C., Ince, N. F., Leuthold, A. C., & Pellizzer, G. (2010). Beta-band activity during motor planning reflects response uncertainty. *The Journal of Neuroscience*, 30, 11270–11277.

- Tzagarakis, C., West, S., & Pellizzer, G. (2015). Brain oscillatory activity during motor preparation: Effect of directional uncertainty on beta, but not alpha, frequency band. Frontiers in Neuroscience, 9, 1-13.
- Veniero, D., Bortoletto, M., & Miniussi, C. (2009). TMS-EEG co-registration: On TMS-induced artifact. Clinical Neurophysiology, 120, 1392-1399.
- Vernet, M., Stengel, C., Quentin, R., Amengual, J. L., & Valero-Cabré, A. (2019). Entrainment of local synchrony reveals a causal role for highbeta right frontal oscillations in human visual consciousness. Scientific Reports, 9, 1-15.
- West, B., Welch, K. B., & Galecki, A. T. (2007). Linear mixed models: A practical guide using statistical software. Chapman & Hall/CRC.
- Yu, Y., Sanabria, D. E., Wang, J., Hendrix, C. M., Zhang, J., Nebeck, S. D., Amundson, A. M., Busby, Z. B., Bauer, D. L., Johnson, M. D., Johnson, L. A., & Vitek, J. L. (2021). Parkinsonism alters beta burst

- dynamics across the basal ganglia-motor cortical network. The Journal of Neuroscience, 41, 2274-2286.
- Zrenner, C., Desideri, D., Belardinelli, P., & Ziemann, U. (2018). Real-time EEG-defined excitability states determine efficacy of TMS-induced plasticity in human motor cortex. Brain Stimulation, 11, 374-389.

How to cite this article: Uehara, K., Fine, J. M., & Santello, M. (2023). Modulation of cortical beta oscillations influences motor vigor: A rhythmic TMS-EEG study. Human Brain Mapping, 44(3), 1158-1172. https://doi.org/10.1002/hbm. 26149